

# CO2PipeHaz Newsletter

Spring 2013

## Introduction

Welcome to the final edition of the EU FP7-funded-project CO2PipeHaz newsletter, highlighting the most recent technical developments. The consortium, led by Prof. Haroun Mahgerefteh at University College London (UCL, UK) comprises 6 other partners: INERIS (France), National Research Centre for Scientific Research (NCSR, Greece), Dalian University of Technology (DUT, PR China), Health and Safety Laboratory (HSL, UK), University of Leeds (UoL, UK) and Gexcon (Norway).

CO2PipeHaz addresses the fundamentally important and urgent issue regarding the accurate predictions of fluid phase, discharge rate, emergency isolation and subsequent atmospheric dispersion during accidental releases from pressurised CO<sub>2</sub> pipelines to be employed as an integral part of large-scale Carbon Capture and Storage (CCS). This information is pivotal to quantifying all the hazard consequences associated with CO<sub>2</sub> pipeline failure, forming the basis for emergency response planning and determining the minimum safe distances to populated areas.

## Message from The Project Coordinator

The CO2PipeHaz project has been a resounding success. Significant progress has been made spanning fundamental theoretical modelling work to the development of unique small and large scale experimental test facilities. Examples of our achievements include the development of an equation of state for CO<sub>2</sub> spanning the supercritical to below the triple point, modelling the impact of craters on the dispersion behaviour of CO<sub>2</sub>, heterogeneous flow modelling, construction of the longest fully instrumented CO<sub>2</sub> test pipeline in China and safe practice guidelines. The above knowledge base, involving seamless collaboration between the project partners and disseminated through over 50 journal publications, presentations at national and international conferences and workshops will enable the safer transportation of CO<sub>2</sub> using pressurised pipelines, thus facilitating the introduction of Carbon Capture and Sequestration as an effective means for combating the impact of global warming.

The success of the CO2PipeHaz project has led to another FP7 project (also lead by UCL), CO2QUEST focussing on the techno-economic assessment of the impact of CO<sub>2</sub> stream impurities on its capture, transportation and storage. This exciting new project, which commenced on 1st March 2013, involves the collaboration of 12 industry and academic partners from Europe, Canada and China. For more information regarding CO2QUEST, please visit:

## CO<sub>2</sub>QUEST

Impact of the Quality of CO<sub>2</sub> on Storage and Transport



## Project Partners



University College London, UK



CMR GexCon, Norway



Dalian University of  
Technology, PR China



Demokritos, National Research Centre  
for Physical Sciences, Greece



Health & Safety Laboratory, UK



INERIS, France



UNIVERSITY OF LEEDS

University of Leeds, UK



# Solid-Fluid Equilibria and Self-diffusion Coefficient Modelling

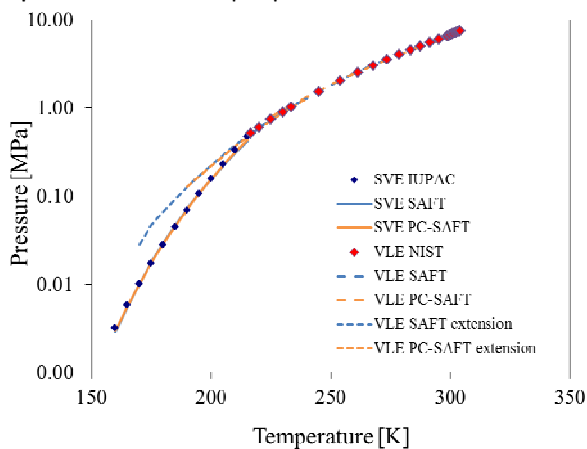
**N. Diamantonis G. Boulougouris, D.M. Tsangaris, and I. Economou**

*National Centre for Scientific Research Demokritos, Greece*

Accurate modelling of solid-fluid equilibria of pure CO<sub>2</sub> is essential when simulating CO<sub>2</sub> pipeline depressurization when conditions below the CO<sub>2</sub> triple point are reached. Here, two fluid-solid models were considered and evaluated:

1. A SAFT/PC-SAFT based model with retuned parameters. This was undertaken in order to predict CO<sub>2</sub> Solid-Vapour Equilibria (SVE) instead of Vapour-Liquid (VLE) Equilibria.
2. A composite model that utilizes an empirical Equation of State for the free energy of solid CO<sub>2</sub> and a variety of classical equations of state for the vapour phase.

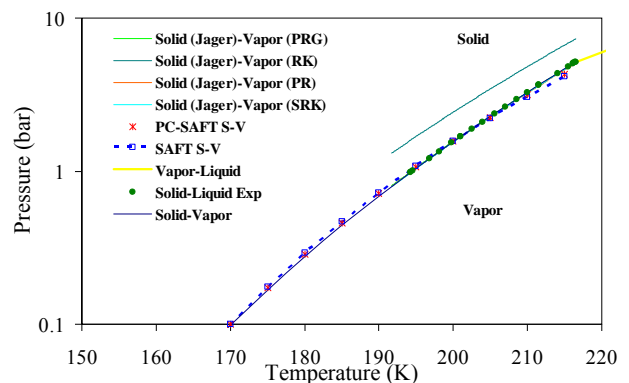
In the first approach, and because the SAFT and PC-SAFT equations of state have been developed and tuned to fluid phase properties (gas, vapour and liquid) model parameters were 'retuned' in order to predict solid-vapour equilibria. Parameter retuning enables SAFT and PC-SAFT to predict solid properties (i.e. density, enthalpy and fugacity) rather than liquid (i.e. solid density in place of liquid density). Thus, when the retuned model is used for equilibria calculations, solid-vapour sublimation properties are obtained.



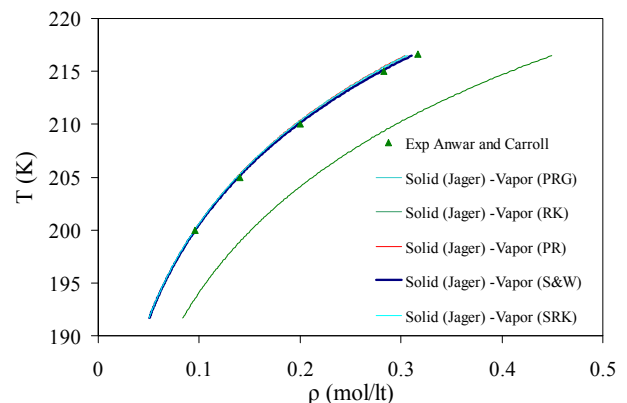
**Figure 1.** CO<sub>2</sub> vapour pressure at temperatures between 160-215 K (SVE) and 215-304 K (VLE). Comparison of different sets of parameters for SAFT and PC-SAFT

Figure 1 indicates that overall good agreement with experimental data can be achieved with this model. It must be emphasized that the retuned equation of state must be used exclusively at temperatures below the triple point.

In the second approach, a composite model which uses the empirical equation for the free energy of the solid proposed by Jager and Span [1] was considered. This equation of state has 23 adjustable parameters which were originally fitted to experimental data of solid heat capacity, molar volume, expansion coefficient and compressibility. In this work, 21 of those parameters were kept at their original values. The remaining two were retuned for each fluid and each equation of state evaluated (SRK, PR, RK) in order to provide thermodynamically consistent models. The new models were used to predict pure CO<sub>2</sub> sublimation properties, and overall good agreement was obtained for all models except the Redlich-Kwong. Representative results for the sublimation pressure are shown in Figure 2 and comparison with the experimental data for the vapour phase density at sublimation is shown in Figure 3.



**Figure 2.** Comparison between model predictions and NIST data for the sublimation pressure of pure CO<sub>2</sub>. Models are based on different cubic EoS and the free energy model of solid CO<sub>2</sub> proposed by Jager and Span



**Figure 3.** Density of the vapour phase at sublimation

The self-diffusion coefficient is a significant property for the efficient design and safe operation of CO<sub>2</sub> transport via pipelines. For the modelling and prediction of the self-diffusion coefficient, two approaches were considered. One based on the Yu and Gao [2] model and one based on the Reis et al. [3] model. Both models are capable of quantitatively reproducing the self-diffusion coefficient at the low gas- and high liquid-density limits.

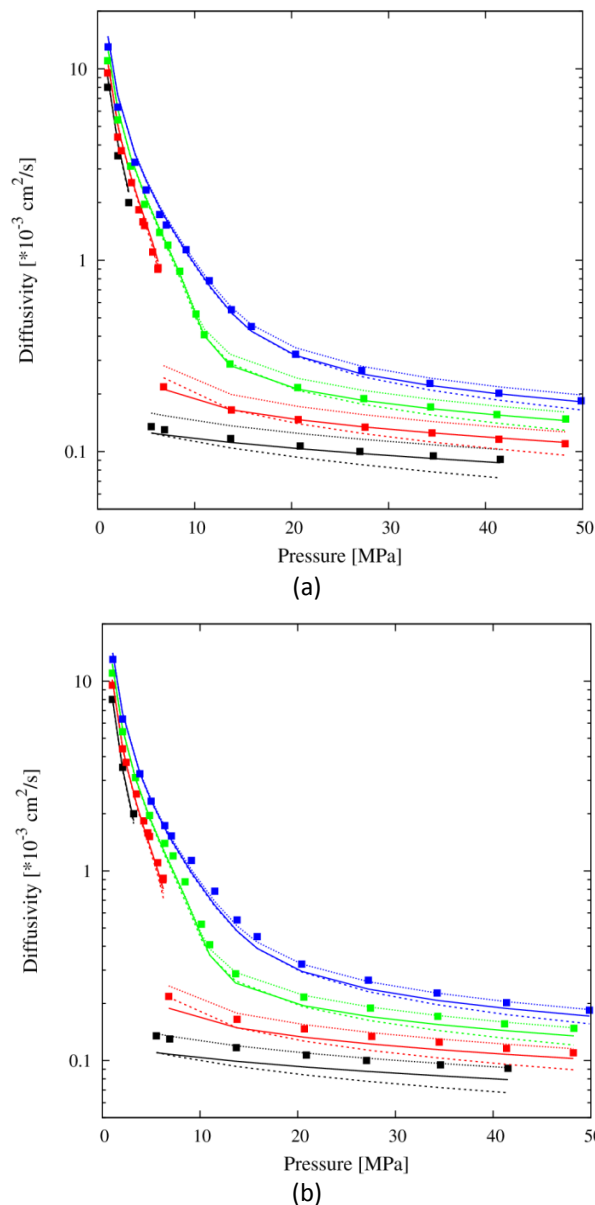


**Figure 4.** Self-diffusion coefficient of pure CO<sub>2</sub>, calculated by (a) Yu and Gao, and (b) Reis et al. models. PC-SAFT (continuous lines), PR (dotted lines), and experimental data [4] (points).

Also In this work, the effect of using different equations of state to account for the pressure dependence of the self-diffusion coefficient for pure CO<sub>2</sub> was evaluated. Figure 4 compares the Peng-Robinson predictions (PR being an

ambassador of cubic equations of state) with the PC-SAFT based predictions. The results indicate that PC-SAFT performs better than PR for the two self-diffusion coefficient models considered in this work. Excellent agreement with the experimental data is achieved with the use of Yu and Gao model.

## Modelling of an Outflow from a CO<sub>2</sub> Pipeline

**S. Martynov, S. Brown and H. Mahgrefteh**

*University College London, UK*

Accurate prediction of CO<sub>2</sub> outflow from an accidentally ruptured or punctured transportation pipeline is central for reliable evaluation of the hazard profile of the system. This requires knowledge of not only the discharge rate and its variation with time, but also of the temperature, pressure and phase composition of the released fluid. The following summarises the findings and advances in outflow modelling that have taken place in WP1.3 as part of CO2PipeHaz.

The results of both small and large-scale experiments conducted by the partners INERIS and DUT have indicated the limitations of the Homogeneous Equilibrium Model (HEM) in simulating outflow following dense phase CO<sub>2</sub> pipeline rupture. This is primarily due to the presence of phase-slip and delayed liquid/vapour phase transition during the rapid depressurisation process, neither of which is accounted for in the HEM. In the case of punctures, visual observation of the in-pipe flow profiles by INERIS has indicated the prevalence of both phenomena. However, in the case of full bore rupture, only delayed phase transition has been found to be prevalent. Hence, as part of WP1.3 of the CO2PipeHaz project a Homogeneous Relaxation Model (HRM) of transient compressible single- and two-phase flow in a pipeline was developed. The model accounts for the thermal non-equilibrium between the vapour and liquid phases during the rapid process of flash vaporization of liquid CO<sub>2</sub> in a depressurising pipeline, which is described using the relaxation equation for the mass

fraction of the vapour phase [5]. Additionally, the flow model developed accounts for the effects of viscous friction and heat transfer, and also has the capability of simulating flow in inclined and segmented pipelines and emergency shutdown isolation [6, 7]. Basic features of the flow model and details of the numerical solution scheme were summarised in the project reports, Deliverable 1.3.1 and Deliverable 1.3.3 [8, 9]

*Formation of any solid CO<sub>2</sub>* resulting from the expansion-induced cooling to below the triple point conditions (5.7 bar, 216.2 K) during the depressurisation process, will significantly alter the CO<sub>2</sub> hazard profile, and hence must be accounted for. Indeed, pipeline rupture tests conducted as part of the CO<sub>2</sub>PipeHaz project have indicated release temperatures as low as 193 K.

*Consequently, a three-phase flow model* for predicting the transient outflow spanning the dense phase to below the triple point has been developed [10]. Depending on the prevailing temperature and pressure, the model is capable of accounting for the solid, vapour and liquid phases in isolation, in pairs, or simultaneously (Figure 5 shows the phase diagram of CO<sub>2</sub>, including the solid region). The choked flow conditions at the rupture plane are modelled through maximisation of the mass flux with respect to pressure, and solids mass fraction at the triple point [11]. The pertinent solid/vapour/liquid phase equilibrium data are predicted through the development of an extended Peng-Robinson equation of state [10].

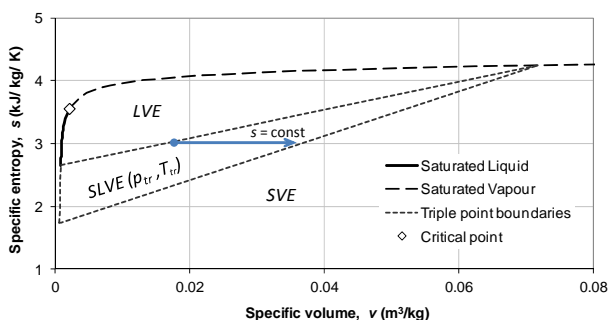


**Figure 5.** CO<sub>2</sub> phase envelope as a function of entropy and specific volume encompassing LVE, SLVE and SVE regions.

*The quality of the equation of state employed* has also been found to have a profound impact on the reliability of the outflow predictions. The outflow model has been coupled to the Physical

Properties Library developed by NCSR Demokritos, which enables the use of various equations of state for CO<sub>2</sub> and its impurities, including H<sub>2</sub>S, N<sub>2</sub>, H<sub>2</sub>O, O<sub>2</sub> and CH<sub>4</sub> (Deliverable 1.2.6). The various equations of state include the highly accurate PC-SAFT, which has been shown to produce improved predictions of phase equilibrium data for CO<sub>2</sub> and its mixtures when compared to the Cubic equations of state. Figure 6 shows an example of the comparison of the pressure predictions obtained with PC-SAFT with experimental data and with Cubic EoS for the shock tube tests conducted by Cosham [12].

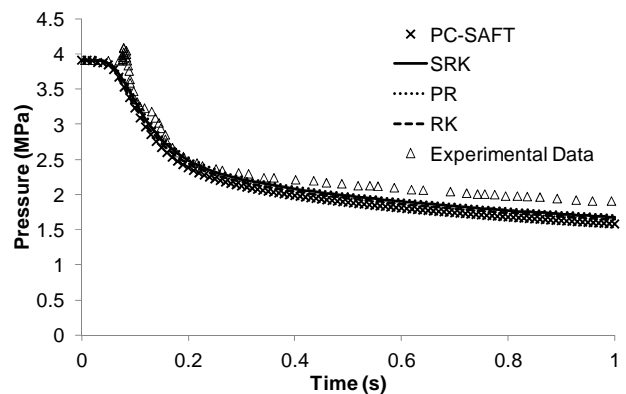


**Figure 6.** Comparison of measured variation of pressure with time with the predictions obtained from PC-SAFT, SRK, PR and RK EoS for a gas phase shock tube release test [12].

## Development of Near-field Dispersion Model

**R.M. Woolley, M. Fairweather, and S.A.E.G. Falle**

*University of Leeds, UK*

The methods and techniques used in the development of the near-field computational fluid dynamic model have been discussed in previous newsletters. Applied methodologies have included: the modification of a two-equation turbulence model to account for the effects of compressibility; modelling of solids-formation within the jet using both a particle equation of motion, and a probability density function approach, accounting for their evolution by means of growth, sublimation, and agglomeration; and inclusion of a composite

equation of state to account for three-phase equilibria.

The final developments to be made to the full 3-dimensional code, and are reported on here, include the inclusion of an advanced Reynolds-stress transport turbulence model, and the coupling of the code to the advanced equations of state developed by partners NCSR. The validation of the code has also been undertaken using recent field-scale data obtained from releases undertaken by partners DUT.

A Reynolds-stress transport model was implemented to represent the effects of turbulence upon the flow-field. The  $k-\epsilon$  model is known to be reasonably reliable for the prediction of axisymmetric jets [13], but is unlikely to do so well for the more complex flows, such as those associated with jets interacting with craters.

A number of possible Reynolds stress models for turbulence have been reviewed by Gatski [14], the main difference between them essentially being the modelling of the redistribution terms for the Reynolds stresses. Here, the model proposed by Jones & Musonge [15] has been implemented for the simple reason the authors have previous experience with this. It is however a simple matter to implement another model, and further investigation is proposed into their relative performances. In the 3-dimensional case, an additional six partial differential equations require solving for the normal and shear stresses.

$\text{CO}_2$  pipeline operating pressures are typically between 30 and 100 bar, depending on the phase being transported, and so will always initially form a highly under-expanded jet at the point of release. The second-moment turbulence model was validated using experimental data of such a highly [16] under-expanded air jet studied by Donaldson and Snedeker [16]. This jet issued from a convergent nozzle, and hence achieved an exit velocity of Mach 1. However, its relatively high nozzle pressure ratio ensures its classification as a highly under-expanded jet.

Figure 7 displays the axial velocity predictions non-dimensionalised with the local sound speed, plotted against the experimental results, for the

highly under-expanded case. The Sarkar [17] compressibility model can be seen to perform relatively well in the representation of the magnitude of Mach number although an under-prediction is observed at the location of the second disk. The phase profile predicted by the Sarkar-modified turbulence model also conforms well to experimental data whereas the standard model becomes non-phased after approximately eight nozzle diameters. The jet decay is also much better represented, demonstrated by conformity with data at twenty five jet diameters downstream. The Reynolds-stress predictions show notable differences to the two-equation model in that the frequency and magnitude of the wave are greater, and the predictions show considerably less dissipative behaviour, which is to be expected.

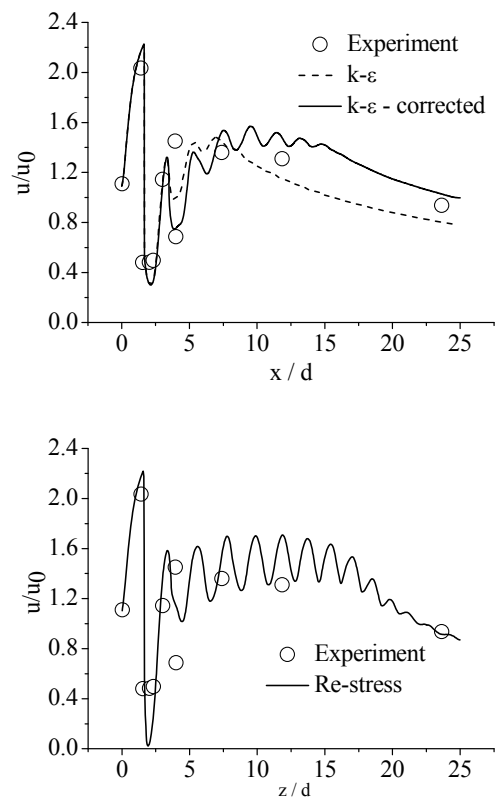


**Figure 7.** Non-dimensionalised axial velocity predictions in the Donaldson and Snedeker air jet (top –  $k-\epsilon$ , bottom – Reynolds stress).

The aim of work undertaken by partners at NCSR, is the development of a Physical Properties Library (PPL) and hence the provision of a 'platform' capable of predicting physical and thermodynamic properties of pure  $\text{CO}_2$  and its mixtures. The PPL contains a collection of models and can be used by all partner models regardless

of scope, type and capabilities (one dimensional homogenous models, near-field CFD, farfield CFD, etc). As previously reported, SAFT and PC-SAFT equations of state have been applied within the PPL to predict thermodynamic properties of pure CO<sub>2</sub> and other gases of interest to CO<sub>2</sub> transportation via pipelines. Calculations have been performed over a wide range of temperature and pressure conditions, and both phase equilibrium and single phase thermodynamic properties were considered, including vapour pressure, liquid density, heat capacities and speed of sound.

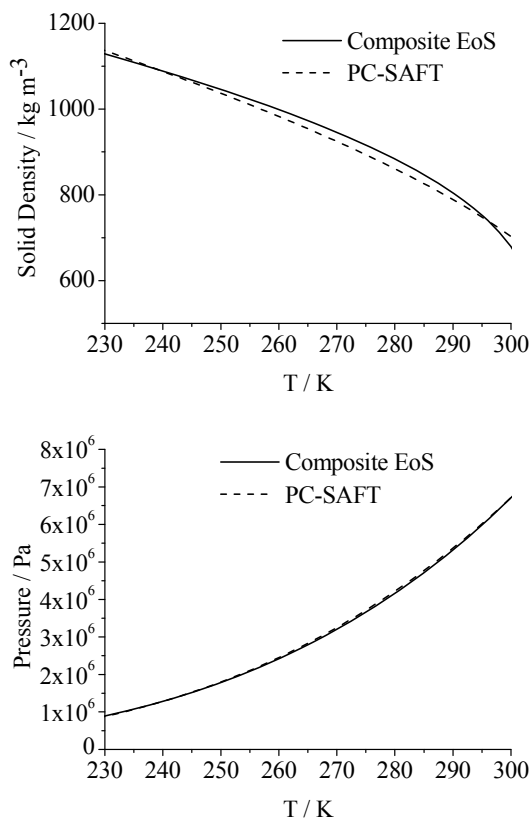


**Figure 8.** Comparison of predicted properties of a pure CO<sub>2</sub> system at saturation.

Figure 8 depicts sample predictions of a pure CO<sub>2</sub> system in equilibrium obtained using PC-SAFT, and also the UoL composite equation of state. The performance of the two models can be seen to be comparable, although discrepancies do appear in some of the derivative quantities such as the dense-phase sound speed. However, these differences appear to have little impact upon the prediction of CO<sub>2</sub> jet structure in the near-field. Figure 9 depicts predictions of two INERIS test-cases undertaken using the composite EoS approach and the PC-SAFT approach developed by NCSR. Plotted are the centreline profiles of

temperature, against experimental observation of the near-field of these two releases. Full descriptions of the experimental procedures, conditions, and results can be found in Deliverables associated with Work Package 2. Effects of physical phenomena such as CO<sub>2</sub> phase transition are clearly observable in the predicted curves. The step-change in gradient of the curve located at the triple-point temperature in Figure 9 is due to the equilibrium transition from liquid-vapour to that of liquid-solid, and the effects of the heat of fusion which is implemented at this point. It is clear that predictions and data are in excellent qualitative and quantitative agreement.

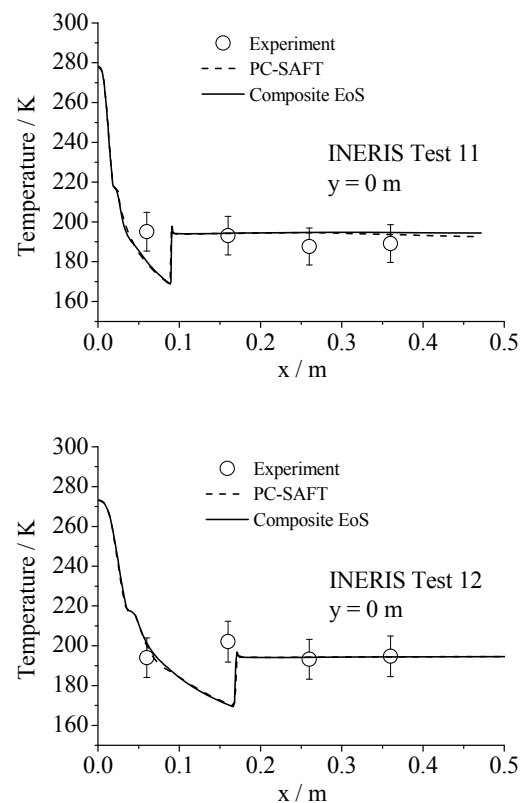


**Figure 9.** Centreline axial prediction of temperature in INERIS test cases 11 and 12, undertaken using the composite equation of state and PC-SAFT approaches.

The final validation of the 3-dimensional model is against data from the large-scale test undertaken by DUT. The test selected for validation purposes was the third test carried out, as at the time, it provided the most comprehensively analysed set of data including initial and release conditions. This particular release was in a pure vapour state at an initial pressure and temperature of 53 bar and 293.15 K respectively. Figure 10 provides sample results from a full 3-dimensional calculation in the form of 2-dimensional slices,

and shows predicted values of turbulence kinetic energy and mean density.

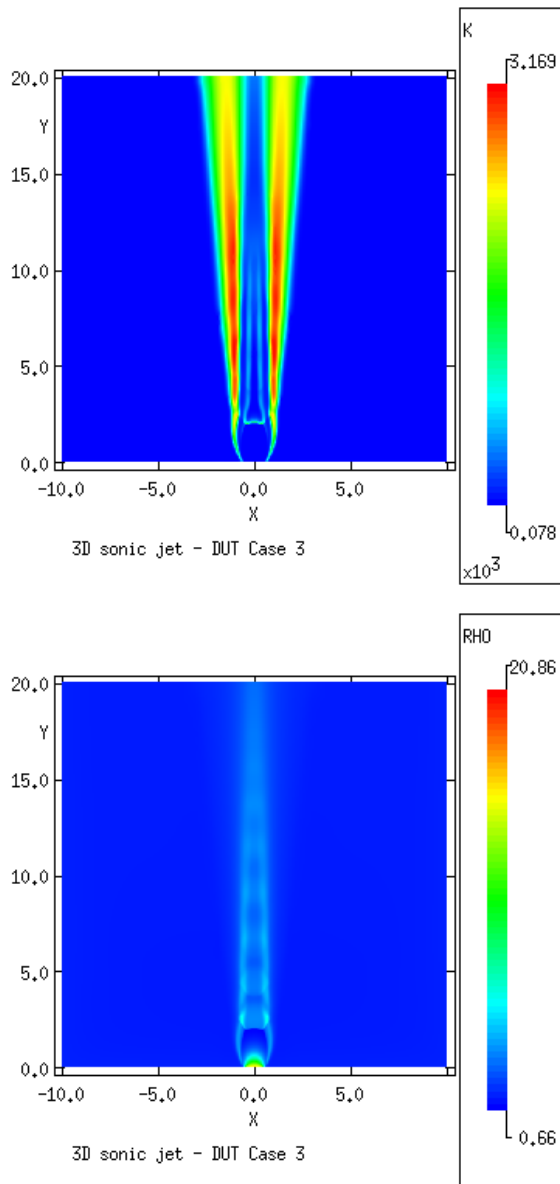


**Figure 10.** 2-dimensional planar plots of mixture turbulence kinetic energy (top), and mean density (bottom) predictions obtained using the 3-dimensional model.

It is evident from this figure that the expected structure of such a highly under-expanded vapour release is well described by the physics embedded within the code. There is a prominent Mach disc observable at approximately 2 nozzle diameters downstream, and at this point, the flow can be seen to have accelerated to over 3.5 times the local sound speed ( $c$ ) which then suddenly drops off as energy is dissipated in the shock region. A subsequent decaying core of shock diamonds is then evident in the predicted densities, extending to approximately 15

diameters downstream. Predictions of turbulence kinetic energy are also in-line with expectation, with the generation occurring due to shear in the high density-gradient region of the jet periphery.

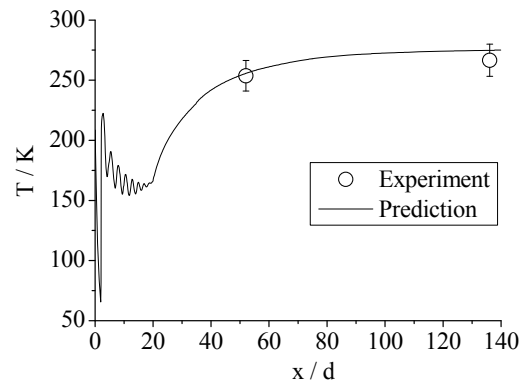


**Figure 11.** Predictions of temperature plotted against experimental data of DUT Test 3, extending to 7 metres downstream (solid curve – predictions, symbols – data)

Figure 11 shows predicted centreline temperatures in the DUT Test 3 case, plotted against experimental observations at 2.6 and 6.8 metres downstream from the release point. No near-field data is available from the large-scale tests for model validation, but by extending the code capability to model further into the far-field permits some comparisons to be made against experiment. As can be seen, the model agrees very well the data at the two locations studied, and alongside the previously presented validations of the near-field model, it can be said that it is capable of accurately describing such releases in detail.

## CO<sub>2</sub> Vapour Dispersion Simulation From Pipeline Release

**V.D. Narasimhamurthy, T. Skjold**

*GexCon AS, Bergen, Norway*

In the current study, the FLACS [18] simulation software was validated using the industrial-scale CO<sub>2</sub> dispersion experiments of partners DUT (WP2.2). As discussed previously in the near-field modelling, DUT test 3 was selected. The DUT experiments consisted of a pipeline of length 260 m containing pure CO<sub>2</sub> at 293.15 K and 53.04 bar. The release orifice diameter ( $d$ ) was 0.05 m and

was located at a height of 0.5 m above the ground, and the ambient temperature was 283.15 K.

DUT test 3 is a pure vapour release without any particles. Therefore, a single-phase gas dispersion problem can be considered. Note that single-phase calculations in FLACS [18] are performed by solving individual transport equations for mixture fraction and mass fraction. A computational domain of 205 m × 200 m × 20 m in the streamwise (X), spanwise (Y) and wall-normal (Z) directions, respectively, is used. This corresponds to approximately 4100 *d* × 4000 *d* × 400 *d*. The time-step ( $\Delta t$ ) was approximately  $10^{-3}$ . In the current study, a fine mesh of about 2.2 million grid points is adopted, where the grid resolution in the jet core region varied from 0.05 m to 0.5 m.

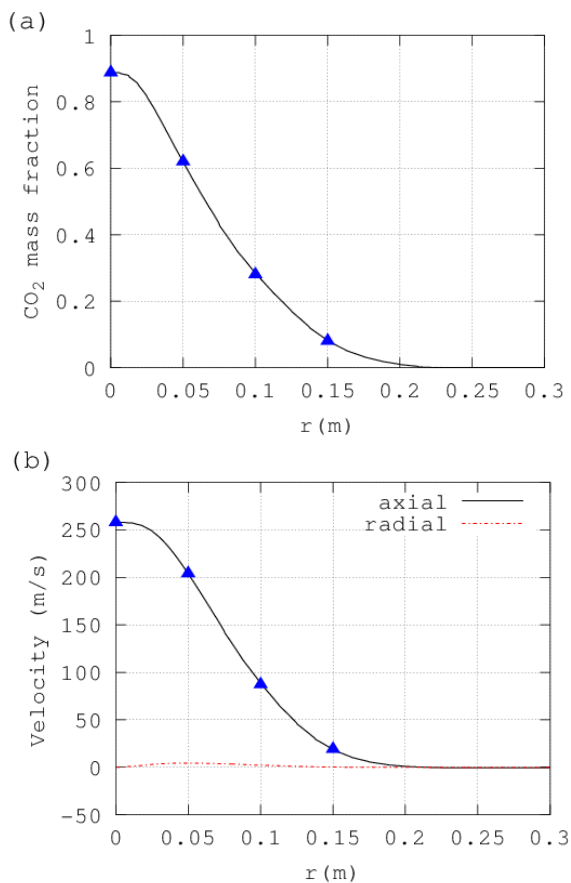


**Figure 12.** Radial variation of the near-field model data in the DUT test 3. Profiles correspond to a location 20 diameter downstream of the orifice. Here symbols represent the point-leak positions in FLACS simulation.

Simulations were performed using an unsteady incompressible solver. Based on the experimental data, wind direction and speed are chosen as 288° and 3.1 m s<sup>-1</sup>, respectively. This wind direction represents an almost side wind. In

addition, Pasquill stability class of type *D* (neutral), where a reference height of 10 m and ground roughness value 0.03 was used. For the wall-boundary condition, the default wall-function in FLACS was employed, and for the outflow boundaries, 'Nozzle' conditions were used to estimate velocity, density and pressure correction coefficient at the boundary nodes. In the current simulation, output from the near-field model from the University of Leeds discussed previously, and as depicted in Figure 12, is applied as source. Note that Figure 12(a) indicates a gaseous mixture of CO<sub>2</sub> and air at all the radial positions. Therefore, the point-leaks in FLACS are given a corresponding mixture fraction value.

Unsteady simulations converged to a steady-state after about 160 seconds of computational time, and Figure 13 shows predicted temperature variation along the jet axis. Results clearly indicate that model predictions are in reasonably good qualitative and quantitative agreement with the experimental data.

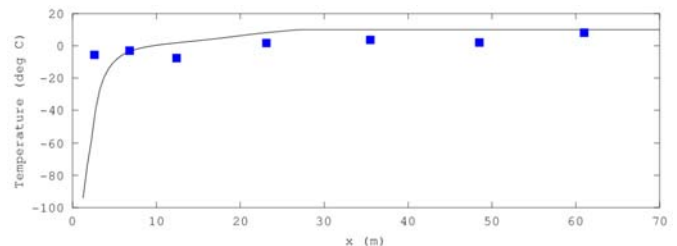


**Figure 13.** Axial variation of temperature (°C) in the far-field simulation (line) of DUT test 3, compared with the time-averaged experimental data (symbol).

## Industrial Scale CO<sub>2</sub> Pipeline Rupture Experiments

**S. Chen, Y. Zhang**

*School of Chemical Engineering, Dalian University of Technology, China*

By the end of the CO<sub>2</sub>PipeHaz project, four field-scale CO<sub>2</sub> release experiments were completed including three 50 mm orifice releases and one full bore rupture (FBR) release. The first industrial pipeline facility in the world for CO<sub>2</sub> release experimentation has, on the whole, proven to be a great success. One of the greatest problems to be overcome considered the arrangement of the

sensor arrays, and the assurance of their integrity. Methods were continually improved to ensure the safety of the instrumentation during the 50 mm releases, and a comprehensive range of experimental data has been obtained. Work remains to be undertaken to improve the measurement methods within the dispersion area for the FBR release as the sheer volume of debris and its associated velocities have proven to be very destructive (Figure 14).



**Figure 14.** Near-field dispersion region during a full-bore rupture.

Important data have been obtained from the four experiments, particularly so for the temperature in the dispersion area for the 50 mm, 52.5 bar and 294 K release. These give an estimation of the CO<sub>2</sub> concentration in the dispersion area via the calculation of the relation between temperature and the released CO<sub>2</sub>. Figure 15 shows the CO<sub>2</sub> concentration along the release axis of the pipeline calculated using these observations.

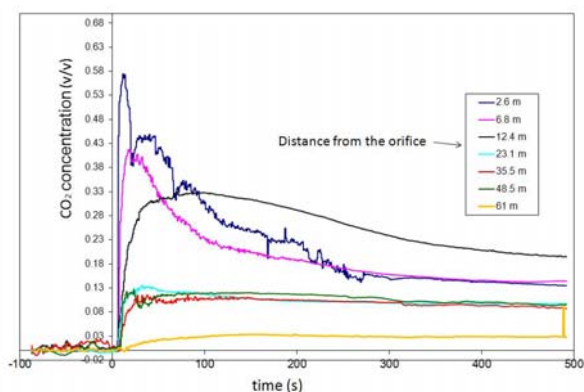


**Figure 15.** CO<sub>2</sub> concentrations at the axis of the CO<sub>2</sub> flow in the different distance from the orifice.

## Pipeline Decision Support Tools

**M.J. Wardman, A.J. Wilday,  
A. McGillivray, S. Gant, J.L. Saw, and  
D. Lisbona**

*Health and Safety Laboratory, UK*

The route of the 30 km hypothetical CO<sub>2</sub> pipeline used is shown in purple in Figure 16, along with the residential populations (brown) and roads (black). For this high pressure pipeline, a set of 24 scenarios [19] were chosen that include a range of potential failures such as full-bore rupture, and large and small holes. Interaction between the release and the ground was also considered in addition to the potential for 'snowout' of any solid CO<sub>2</sub> that is created. The discharge and dispersion calculations were carried out using Phast version 6.7 [20], a commercially available integral model which has recently been enhanced to allow the effects of solid CO<sub>2</sub> to be considered.

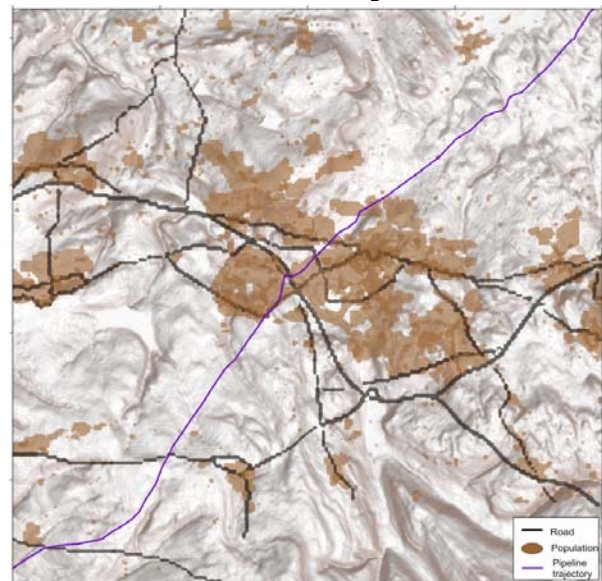


**Figure 16.** 30km test-case pipeline route

HSE's QuickRisk tool [21] was used to calculate the individual and societal risks associated with the pipeline. The tool allows an extended range of scenarios to be defined and it makes use of the National Population Database (NPD) [22, 23] which contains detailed population data for residential, workplace and road locations. Failure rates and weather conditions were also input to the tool.

### Individual risk

Figure 17 shows a range of individual risk results, including standard risk contours, and also

location specific risk transects. The pipeline route is shown in purple, and is a subsection of the same pipeline defined in Figure 16.

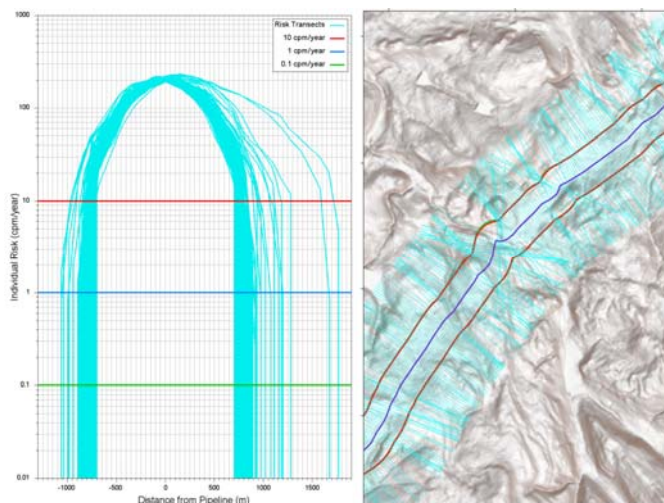


**Figure 17.** Risk transects at regularly spaced points along the pipeline route

The right hand side of Figure 17 gives the individual risk contours for three risk levels, 0.1 (green), 1 (dark blue) and 10 (red) chances per million (cpm)/year. The 1 cpm/year contour corresponds to the lower level in the HSE criteria for individual risk of fatality, but any appropriate risk criteria levels can be used. Figure 17 shows that an 'exclusion corridor' is created for individual risk along the length of the pipeline rather than the traditional zones that are produced for substances such as methane. This is because the dose relationship for CO<sub>2</sub> is highly dependent on the concentration and results in this cliff edge effect where the zones are indistinguishable. This effect means that accurate dispersion results are required to prevent the risks being over- or under-predicted, and subsequently a specified corridor that is too wide or too narrow. The contours show the extent of risk on either side of the pipeline and could be used to control developments within the zones.

The left hand side of Figure 17 shows the risk transect results which correspond to the blue cross sections perpendicular to the pipeline on the right hand image. The transects can be compared against appropriate risk criteria, in this case 0.1, 1 and 10 cpm/year as before. Depending on the risk criteria used, locations with unacceptable levels of risk can be identified using risk transects, and where appropriate, risk reduction and re-routing of the pipeline to avoid these populated areas may be required.

### Societal risk

Societal risk results take into account existing population. Several layers of population are used, including day and night residential populations, roads, and workplaces. The various combinations over each time period are taken into account in the calculations.

Figure 18 shows FN curves for two segments from the pipeline as indicated on the map. In this case it can be seen that one is above the criterion line [24] and one is below. This means that further risk reduction for the green segment needs to be considered, and an ALARP demonstration provided.

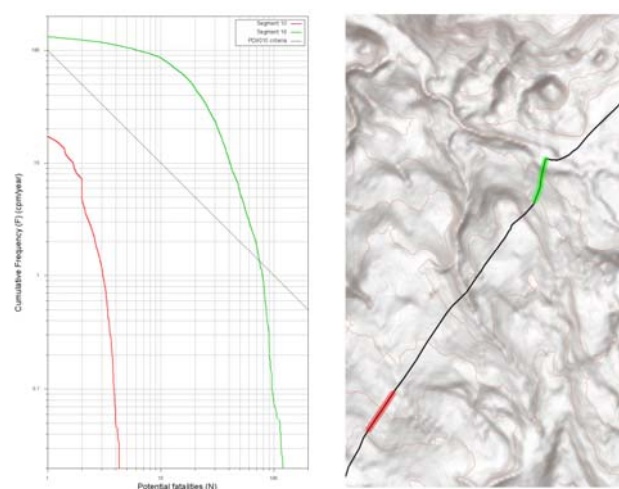


**Figure 18.** FN curve for two 1km pipeline segments

## References

1. Jager, A. and R. Span, *Equation of State for Solid Carbon Dioxide Based on the Gibbs Free Energy*. Journal of Chemical and Engineering Data, 2012. **57**: p. 590-597.
2. Yu, Y.-X. and G.-H. Gao, *Self-diffusion coefficient equation for polyatomic fluid*. Fluid Phase Equilibria, 1999. **166**: p. 111-124.
3. Reis, R.A., et al., *Self- and mutual diffusion coefficient equation for pure fluids, liquid mixtures and polymeric solutions*. Chemical Engineering Science, 2005. **60**: p. 4581-4592.
4. Etesse, P., J.A. Zega, and R. Kobayashi, *High pressure nuclear magnetic resonance measurement of spin-lattice relaxation and self-diffusion in carbon*

- dioxide*. The Journal of Chemical Physics, 1992. **97**(3): p. 2022-2029.
5. Brown, S., et al., A *Homogeneous Relaxation model for CO<sub>2</sub> pipeline decompression*. Journal of Chemical Engineering Science, 2013. **(in review)**.
  6. Mahgerefteh, H., P. Saha, and I. Economou, *Modeling Fluid Phase Transition Effects on Dynamic Behavior of ESDV*. American Institute of Chemical Engineers Journal, 2000. **46**(5): p. 997-1006.
  7. Mahgerefteh, H., S. Brown, and S. Martynov, *A study of the effects of friction, heat transfer, and stream impurities on the decompression behavior in CO<sub>2</sub> pipelines*. Greenhouse Gases: Science and Technology, 2012. **2**: p. 369-379.
  8. Martynov, S., *A report describing detailed formulation of the conservation equations and the finite volume numerical solution scheme*. Deliverable 1.3.1 CO<sub>2</sub>PipeHaz project, University College London: Deliverable 1.3.1 CO<sub>2</sub>PipeHaz project. 2011.
  9. Martynov, S., *A validated heterogeneous discharge model*. Deliverable 1.3.3 CO<sub>2</sub>PipeHaz project, University College London: Deliverable 1.3.3 CO<sub>2</sub>PipeHaz project. 2013.
  10. Martynov, S., et al., *Modelling choked flow conditions for CO<sub>2</sub> around its triple point*. International Journal of Multiphase Flow, 2013. **(to appear)**.
  11. Martynov, S., S. Brown, and H. Mahgerefteh, *An Extended Peng-Robinson Equation of State for Carbon Dioxide Solid-Vapour Equilibrium*. Greenhouse Gases: Science and Technology, 2013. **3**(2): p. 136-147.
  12. Cosham, A., et al. *The decompression behaviour of CO<sub>2</sub> in the gas phase*. in *International Forum on the Transportation of CO<sub>2</sub> by Pipeline*. 2011. June 22-23 Newcastle upon Tyne.
  13. Cumber, P.S., et al., *Predictions of the Structure of Turbulent, Highly Underexpanded Jets*. Journal of Fluids Engineering, 1995. **117**: p. 599-604.
  14. Gatski, T.B., *Constitutive equations for turbulent flows*. Theoretical Computational Fluid Dynamics, 2004. **18**: p. 345-369.
  15. Jones, W.P. and P. Musonge, *Closure of the Reynolds stress and scalar flux equations*. Physics of Fluids, 1988. **31**(12): p. 3589-3604.
  16. Donaldson, C.D., R.S. Snedeker, and D.P. Margolis, *A study of free jet impingement. Part 2. Free jet turbulent structure and impingement heat transfer*. Journal of Fluid Mechanics, 1971. **45**(3): p. 477-512.
  17. Sarkar, S., et al., *The analysis and modelling of dilatational terms in compressible turbulence*. Journal of Fluid Mechanics, 1991. **227**: p. 473-493.
  18. GexconAS. *FLACS v9.1 User's Manual*, 2011. 21/02/13; Available from: <http://www.flacs.com>.
  19. McGillivray, A., et al., *A risk assessment methodology for high pressure CO<sub>2</sub> pipelines using integral consequence modelling*. Process Safety and Environmental Protection, 2013. **(to appear)**.
  20. DNV, *Phast Release Notes for V6.7*. 2011.
  21. Wardman, M., et al. *QuickFN: a simplified methodology for societal risk estimates*. in *Proceedings of the 12th International Symposium on Loss Prevention and Safety Promotion in the Process Industries*. 2007. IChemE Symposium Series No. 153.
  22. Smith, G., et al., *A National Population Data Base for Major Accident Hazard Modelling'*. HSE Research Report 297, HSE Books: Sudbury. 2005.
  23. Smith, G. and J. Fairburn, *Updating and Improving the National Population Database to National Population Database 2*. HSE Research Report 678, HSE Books: Sudbury. 2008.
  24. B.S.I., *Code of practice for pipelines. Steel pipelines on land. Guide to the application of pipeline risk assessment to proposed developments in the vicinity of major accident hazard pipelines containing flammables*. Supplement to PD 8010-1:2004, PD 8010-3:2009, 2009, British Standards Institution.

## Publications and Conference Participation

For regular updates on publications please visit:

<http://www.co2pipehaz.eu/publications.htm>

The most recent CO2PipeHaz event was the multi-disciplinary **'Bridging the gap in CCS infrastructure: Results from European projects'** meeting held in Lisbon, Portugal. All presentations will be available for download from the project website in due course

In addition to CO2PipeHaz, the meeting was co-organised by two major CCS infrastructure projects COMET, and COCATE. A wide range of material was presented and discussed by both academic and industrial contributors, and this material will be subsequently published as a special edition of a leading peer reviewed journal. Again, please monitor the project website for the latest developments.

A number of papers, posters, and presentations are available in the publications section of the project website.

## Acknowledgement and Disclaimer

The authors gratefully acknowledge funding received from the European Union 7<sup>th</sup> Framework Programme FP7-ENERGY-2009-1 under grant agreement number 241346.

The newsletter reflects only the authors' views and the European Union is not liable for any use that may be made of the information contained therein.